

2007

Semiconductor photonic integration using quantum nanostructure interdiffusion

Vitchanetra Hongpinyo
Lehigh University

Follow this and additional works at: <http://preserve.lehigh.edu/etd>

Recommended Citation

Hongpinyo, Vitchanetra, "Semiconductor photonic integration using quantum nanostructure interdiffusion" (2007). *Theses and Dissertations*. Paper 966.

This Thesis is brought to you for free and open access by Lehigh Preserve. It has been accepted for inclusion in Theses and Dissertations by an authorized administrator of Lehigh Preserve. For more information, please contact preserve@lehigh.edu.

Hongpinyo,
Vitchanetra

Semiconductor
Photonic Integration
Using Quantum
Nanostructure
Interdiffusion

May 2007

**Semiconductor Photonic Integration Using Quantum
Nanostructure Interdiffusion**

by

Vitchanetra Hongpinyo

A Thesis

Presented to the Graduate and Research Committee

of Lehigh University

in Candidacy for the Degree of

Master of Science

in

Department of Electrical and Computer Engineering

Lehigh University

May 2007

This thesis is accepted and approved in partial fulfillment of the requirements for the Master of Science.

04/25/2007

Date

(Boon Siew Ooi)

Thesis Advisor

(Filbert J. Bartoli)

Chairperson of Department

ACKNOWLEDGEMENTS

There are so many people who played important roles in the completion of this thesis, and encouraged me throughout the whole process. This work will not be done if I don't have support from the most two important persons, my advisor, Associate Professor. Boon Siew Ooi and the group's post-doc, Dr. Hery Susanto Djie. They were always there to teach me all the experimental skills I need, and patiently answer my questions and guide me in the right directions during all the experimental works. In addition, I would like to thank the Center for Optical Technologies for providing all the facilities for the experiments.

I would like to thank all my friends and especially my family who helped me and supported me even when I have struggled with the work. Last but not least, my sincere thanks to all research students working in the same laboratory who have kindly lent me helping hands in one way or another.

TABLE OF CONTENTS

| | |
|------------------------------|----|
| Abstract..... | 1 |
| Introduction..... | 3 |
| Experimental Procedures..... | 16 |
| Results..... | 27 |
| Discussion..... | 43 |
| Conclusions..... | 44 |
| References..... | 46 |
| Vita..... | 48 |

LIST OF FIGURES

Chapter 1

Figure 1-1 Schematic of quantum well intermixing, and the bandgaps of the as-grown and the intermixed quantum nanostructures.

Figure 1-2 The schematic diagram of the sputtering system.

Figure 1-3 Radio Frequency Sputtering System.

Figure 1-4 Basic components of XPS system.

Chapter 2

Figure 2-1 (a) The schematic representation of the GaAs/AlGaAs DQW layer structure and (b) its Photoluminescence at 4K and 77K .

Figure 2-2 (a) The schematic representation of the InGaP/GaAs SQW layer structure and (b) Schematic representation of the GaAs/AlGaAs SQW layer structure.

Figure 2-3 Rapid Thermal Processor (RTP) using in this project.

Figure 2-4 The schematic diagram of the 77K PL setup.

Figure 2-5 The 77K PL system.

Figure 2-6 The sputtering system.

Figure 2-7 Alpha Step Surface Profiler.

Chapter3

Figure 3-1 The PL spectra at 77K after rapid thermal annealing at various temperatures [(i) 875 °C, (ii) 900 °C, (iii) 925 °C, and (iv) 950 °C] from (a) the bare (note that the spectrum of as-grown is included as the dotted line), (b) SiO₂ capped GaAs/AlGaAs 2×10^{12} cm⁻² of copper ion implanted QWs material.

Figure 3-2 The PL spectra at 77K after rapid thermal annealing at various temperatures [(i) 875 °C, (ii) 900 °C, (iii) 925 °C, and (iv) 950 °C] from (a) the bare (note that the spectrum of as-grown is included as the dotted line), (b) SiO₂ capped GaAs/AlGaAs 5×10^{13} cm⁻² of copper ion implanted QWs material.

Figure 3-3 The PL spectra at 77K after rapid thermal annealing at various temperatures [(i) 875 °C, (ii) 900 °C, (iii) 925 °C, and (iv) 950 °C] from (a) the bare (note that the spectrum of as-grown is included as the dotted line), (b) SiO₂ capped GaAs/AlGaAs 2×10^{15} cm⁻² of copper ion implanted QWs material.

Figure 3-4 The PL energy shifts measured at 77K versus annealing temperature from SiO₂ capped GaAs/AlGaAs QWs samples at various copper dosages.

Figure 3-5 The PL spectra at 77K after rapid thermal annealing at various temperatures [(i) 875 °C, (ii) 900 °C, (iii) 925 °C and (iv) 950 °C (note that the spectrum of as-grown is included as the dotted line)] from co-sputtered Cu:SiO₂ GaAs/AlGaAs QWs materials.

Figure 3-6 The PL spectra at 77K after rapid thermal annealing at various temperatures [(i) 800 °C, (ii) 850 °C, (iii) 900 °C, and (iv) 925 °C] from co-sputtered Cu:SiO₂ single quantum well InGaP/GaAs red laser material.

Figure 3-7 The PL spectra at 77K after rapid thermal annealing at various temperatures [(i) 700 °C, (ii) 750 °C, (iii) 775 °C, and (iv) 800 °C] from co-sputtered Cu:SiO₂ AlGaAs/GaAs quantum well laser (780nm).

Figure 3-8 The PL energy shifts measured at 77K versus annealing temperature from sputtered GaAs/AlGaAs QW, InGaP/GaAs red laser material, and AlGaAs/GaAs quantum well laser (780nm).

Figure 3-9 X-ray Photoelectron Spectroscopy from copper implanted GaAs based bare samples before rapid thermal annealing. (a) Overall signal from the sample (b) Zoom in binding energy peak obtains from copper element (note that copper binding energy peak is around 932-933 eV).

Figure 3-10 X-ray Photoelectron Spectroscopy from copper implanted samples after rapid thermal annealing. (a) Overall signal from the sample (b) Zoom in binding energy peak obtains from copper element (932-933 eV).

Figure 3-11. X-ray Photoelectron Spectroscopy from co-sputtered Cu:SiO₂ samples after removing SiO₂ layer before rapid thermal annealing. (a) Overall signal from the sample (b) Zoom in binding energy peak obtains from copper element (932-933 eV).

Figure 3-12. X-ray Photoelectron Spectroscopy from co-sputtered Cu:SiO₂ samples after removing SiO₂ layer after rapid thermal annealing. (a) Overall signal from the sample (b) Zoom in binding energy peak obtains from copper element (932-933 eV).

ABSTRACT

Monolithic integrated circuits (PICs) and optoelectronic integrated circuits (OEICs) have been a goal actively pursued since early 60s. Over the years, there are several viable technologies developed for monolithic PICs. These technologies include (i) selective area epitaxy, (ii) growth and regrowth, (iii) asymmetric waveguide structure, and (iv) quantum well intermixing (QWI). In this thesis, we investigate the feasibility of using Cu:SiO₂ film to induce QWI for GaAs-based quantum well systems.

Intermixing is a technique that can be used to modify the band gap of QW laser structures. The spatial selectivity inherent in this technique makes it useful for the monolithic integration of optoelectronic devices having different functionalities. This process offers a simple and potentially low-cost route for the fabrication of photonic integrated circuits. To date, several promising QW intermixing (QWI) techniques has been developed. These techniques have shown to increase the production yield and performance of photonic integrated circuits (PICs).

Here, we systematically investigate the possible influence of metallic impurity incorporation into the silica encapsulating layer through ion implantation and co-sputtering technique to enhance the intermixing rate in the various quantum nanostructure systems. In our study, we found that the interdiffusion rate can be controlled by incorporating different concentration of copper (Cu) in the silica cap through either co-sputtering of Cu and SiO₂, or Cu-implanted SiO₂ process. Large bandgap shift of over 200 meV has been observed from various QW heterostructures such as GaAs/AlGaAs

QW laser (850nm), InGaP/GaAs red laser (633nm) structure and AlGaAs/GaAs quantum well laser structure (780nm) using Cu-doped sputtered silica process. The results suggest that this technology is a promising universal intermixing technique for the planar integration of multiple active/passive quantum heterostructure based devices on a single chip.

CHAPTER 1

INTRODUCTION

1.1 Motivation

Engineering of optical and material properties of semiconductor quantum confined nanoheterostructures using interdiffusion or intermixing technology has gained significant interest. This technique provides a simple and cost effective route to the realization of monolithic semiconductor photonic integrated circuits (PICs) which allows active and passive photonic devices such laser, modulators, photodetector and low loss waveguides to be fabricated on a single chip. By intermixing the quantum-well and barrier materials, the absorption, emission, and refractive properties can be controlled. In addition, this technique produces excellent alignment, negligible reflection losses, and intrinsic mode matching between integrated devices, hence providing a very enticing vision for the future of high-density PICs. The process takes an advantage of the inherent metastable III-V compound semiconductor to spatially modify the material bandgap via the introduction of beneficial impurities or point defects followed by a thermal annealing stage. Among the well-established intermixing techniques (i.e. dielectric cap annealing, ion-implantation, impurity diffusion, laser irradiation, plasma exposure), sputtered silica process has been widely known as a promising and reliable approach to universally tune the bandgap of various quantum nanoheterostructures such as quantum-well (QW) and quantum-dot (QD) [2]. However, the intermixing mechanism of the sputtered silica

process is not well understood. Also, the present knowledge is insufficient to explain why the intermixing effect occurs at relatively low activation energy as compared to other processes.

1.2 Quantum Nanostructure (quantum well or quantum dot) Intermixing

Quantum Well Intermixing

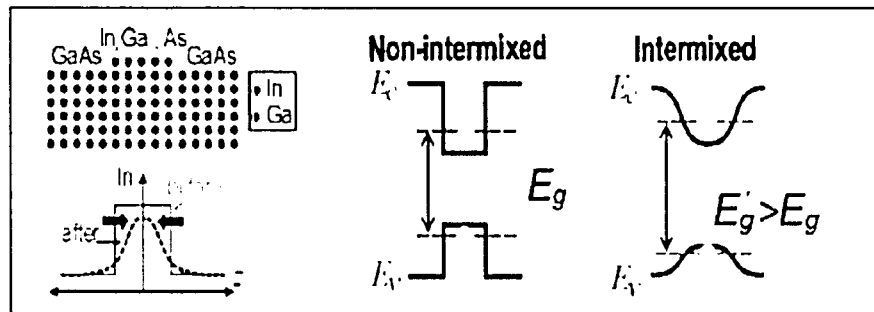


Figure 1-1 Schematic of quantum well intermixing, and the bandgaps of the as-grown and the intermixed quantum nanostructures.

Quantum well intermixing (QWI) is a technique that can be applied to spatially modify the bandgap of the active quantum nanostructure in semiconductor photonic structures (Figure 1-1). The modified quantized energy state is usually observed as a blue-shift of the band edge, that is, an increase in the quantized energy state. Hence provides a route for the monolithic integration of various optical components that required different bandgap properties onto a single semiconductor wafer. Intermixing technique offers a planar technology which can be used to laterally integrate regions of

different bandgaps within the same epitaxial layer. Generally, the interface between quantum well and barriers is metastable. At high annealing temperature, interdiffusion between elemental atoms in the quantum well and barrier occurs that modifies the composition of the quantum well, hence the bandgap of the active region.

By intermix the quantum well and barrier materials, optical properties of the active region such as absorption, emission, and refractive properties can be controlled. This process offers a simple and low-cost route for the fabrication of photonic integrated circuits (PICs). This planar technology will also increase device yield and the performance of PICs. A range of intermixing techniques has been reported, based on impurity diffusion, dielectric capping, ion-implantation, laser irradiation and plasma exposure has been developed to enhance the quantum well intermixing rate in selected areas of a wafer. Each of these QWI techniques has its advantages and shortcomings.

1.2.1 Impurity Induced Disordering (IID)

Among all of the QWI methods, impurity induced disordering (IID) is a process that requires the introduction of impurities into the QW materials in order to promote the intermixing process. It was first observed and demonstrated in the AlAs/GaAs by Laidig et al [6] in 1981. Later, the mechanism of IID in GaAs/AlGaAs was then proposed by Deppe and Holonyak [7].

In the impurity-induced disordering (IID) method, impurities, both electrically active and neutral species, are used to change the equilibrium defect concentration to enhance the group III or group V self-diffusion in the crystal during high temperature annealing. Although the technique has shown to be relatively simple and highly reproducible, the introduction of dopants in to the epi-structures could have adverse effects on the electrical nature of the device structure [3].

1.2.2 Impurity Free Vacancy enhanced Disordering (IFVD)

Impurity-free vacancy-enhanced disordering (IFVD) is another commonly used technique to induce QWI. In the case of IFVD, dielectric cap such as SiO_2 is usually used as the intermixing source to create surface point defects particular vacancies, hence QWI at high annealing temperature. Take a simple GaAs/AlGaAs QW structure for example, SiO_2 encapsulant layer induce Ga outdiffusion, i.e., Group III vacancies, during annealing. These vacancies will diffuse toward the QW structure and enhance the atomic interdiffusion rate between QW and barrier materials, hence induce QWI to the structure. The outdiffusion of group III elements to the SiO_2 layer has been attributed to the large thermal expansion coefficient of between the semiconductor and SiO_2 . As the thermal expansion coefficient of GaAs is ten times larger than that of SiO_2 , the thermal stress at the interface between the GaAs and the SiO_2 layer plays a major role. During high temperature annealing, the bonding in the porous SiO_2 may be broken due to the stress gradient between the GaAs and SiO_2 film. Thus, the outdiffuse of Ga occurs and helps to relieve the tensile stress in the GaAs. Also, As atoms might diffuse into SiO_2 as well. However, since the diffusion coefficient of As in SiO_2 is utterly low compared to Ga, Ga will dominate the out diffuse.

Although IFVD is one of the most promising QWI techniques for GaAs/AlGaAs system, this technique produce low spatial selectivity and low reproducibility in InP-based material systems.

1.2.3 Laser Induced Disordering (LID)

Laser-induced disordering (LID) technique involves heating up the quantum well structure through laser irradiation to accomplish QWI. It is a promising QWI process for InGaAs/InGaAsP QW systems due to the poor thermal stability in InGaAsP material. This technique was first demonstrated in a GaAs/AlGaAs structure using a CW Ar laser irradiation technique [8]. Large thermal spike from the CW laser irradiation results in melting of semiconductor, hence modifying of the bandgap property of the active structure. Generally, this technique gives low spatial selectivity, and induces warble to the sample.

1.3 Sputtering Deposition or Physical Vapor Deposition (PVD) Review

1.3.1 Sputtering Mechanism

Sputtering deposition which also known as physical vapor deposition (PVD) is process widely used for depositing thin film of material on semiconductor substrates. Typically the layers are used as diffusion barriers, adhesion or seed layers, primary conductors, anti-reflection coatings, and etch stops in the semiconductor manufacturing. Physical sputtering has been known for more than a hundred years and has been in common usage for many decades [14]. Physical sputtering is a relatively aggressive, atomic-scale process in which an energetic ion bombards a material or a “target” which made of the material to be deposited. As a result, the target atoms will be dislodged or “sputtered” off. The sputtered atoms will then have enough substantial kinetic energies to fly to the substrate and coated on it as shown in Figure 1-2.

The degrees of the collision process depend directly on the incident energy and mass of the bombarding particles. At relatively low energies, the incident particles do not have enough energy to break atomic bonds of the surface atoms, and the bombardment process could result in simply desorbing a few lightly bound gas atoms and may ends up inducing a chemical reaction at the sample surface, or nothing at all. On the other hand, at relatively high energies, the bombarding particles travel deeply into the substrate and may also cause deep level disorder in the physical structure. At moderate energies, usually in the range from several hundred eV to several keV, the bombarding particles

can cause considerable numbers of near surface broken bonds, atomic dislocations and sputtering atoms.

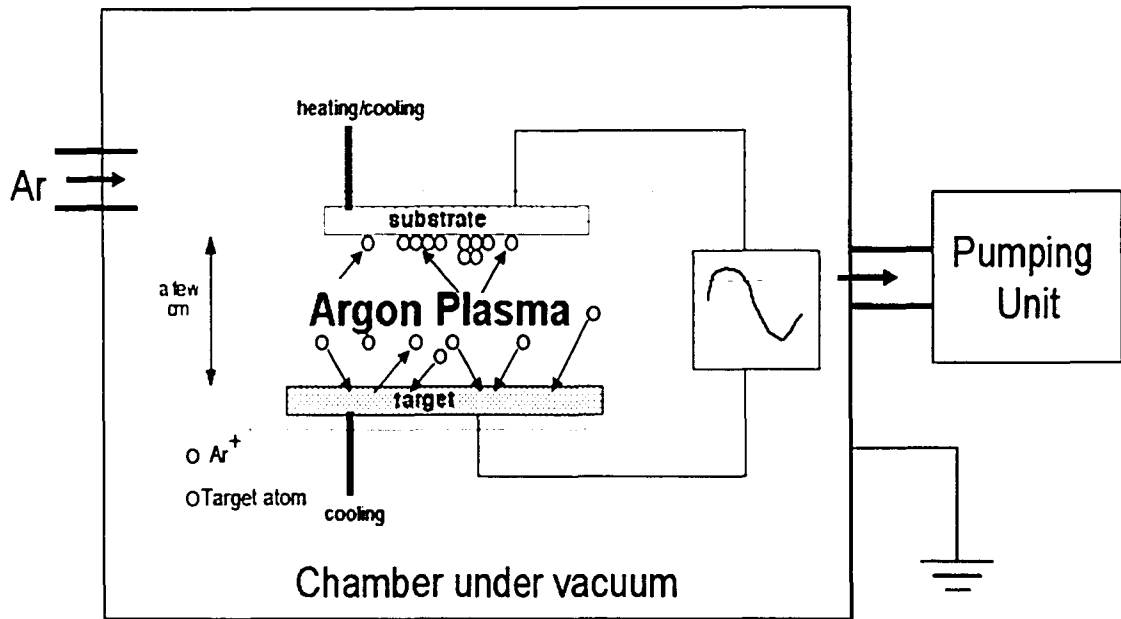


Figure 1-2. The schematic diagram of the sputtering system.

Most of the ions necessary for the bombardment of the target are simply extracted from inert sputtered gas which is typically Argon plasma, burning between the target and the substrate. Both target and substrate are planar plates which serve as the cathode and anode for the gas discharge that produces ionized Ar^+ and free electrons. Since the target electrode is always cathode which is negatively charged, it will attract the Ar^+ ions and thus is bombarded by relatively energetic Ar^+ ions. Moreover, some target atoms will make it to the substrate to be coated, others will miss it, and some will become ionized and return to the target. Sputtering offers lots of advantages as following

- Sputtering can be achieved from large-size targets, simplifying the deposition of film with uniform thickness over large wafers.
- The film thickness is easily controlled by fixing the operation parameters and simply adjusting the deposition time.
- The control of the alloy composition, as well as other film properties such as step coverage and grain structure, is more easily accomplished than by deposition through evaporation.

However, sputtering has the following disadvantages too:

- High capital expenses are required
- The rates of deposition of some materials such as SiO_2 are relatively low
- Some materials such as organic solids are easily degraded by ionic bombardment
- Sputtering has a greater tendency to introduce impurities in the substrate than deposition by evaporation because the former operates under a lesser vacuum range than the latter.

1.3.2 Radio-Frequency (RF) sputtering

RF sputtering system uses a RF generator to produce a signal of alternating polarity that is large enough to cause breakdown of the process chamber gas. Positive ions from the discharge are accelerated toward an electrode when it is subjected to the negative-bias portion of the waveform (and electrons during the positive-bias portion). To restrict the sputtering only to the target surface, the electrode

configuration in the system must be altered. The non-sputtering electrode is grounded, and this may also be a convenient location for placing the substrate wafers onto which the sputtered film is to be deposited. If the target is a conductor, a blocking capacitor is needed to prevent this self-bias voltage from being grounded through the RF generator as shown in Figure 1-3. If the target were an ideal insulator, it would not be necessary to use an external blocking capacitor.

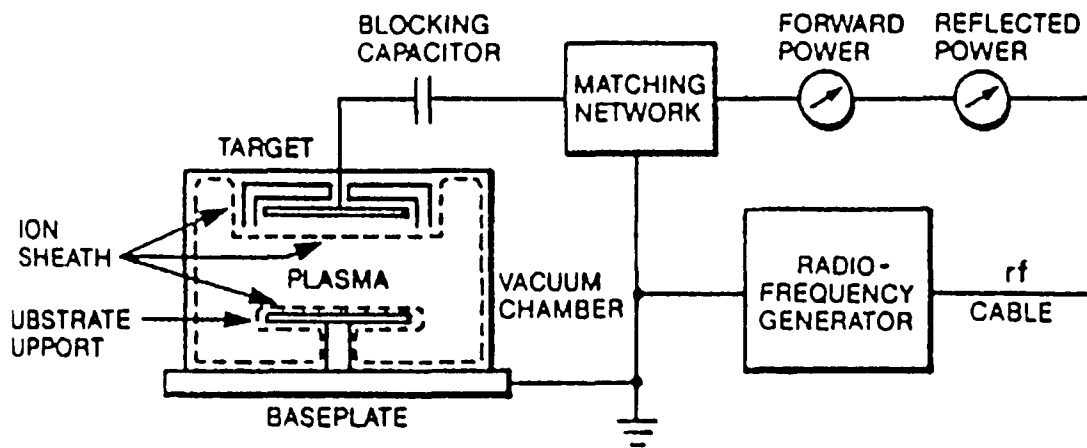


Figure 1-3. Radio Frequency Sputtering System

However, one of the important requirements that must be met to realize a useful RF sputter process is to be able to couple the maximum power from the RF generator to the discharge. The output impedance, Z_0 , of RF power supplies used in sputtering is designed to be purely resistive while the load of the discharge X_L is much larger and the impedance is also largely capacitive. This impedance mismatch can be solved by inserting an impedance matching network between the output of the generator and

discharge chamber. Most RF systems use feedback control to tune to network by automatically maintaining minimum reflected power.

1.4 X-ray Photoelectron Spectroscopy (XPS)

X-ray photoelectron spectroscopy (XPS) or also called electron spectroscopy is a method that uses x-rays to eject electrons from inner-orbital shells. It was developed in the mid 1960s by Kai Siegbahn and his research group. It is a technique that used to analyze the surface chemical property of a material. Typically, it is used to analyze the chemical composition of a surface after some treatment such as: fracturing, cutting or scraping in air, ion beam etching (surface cleaning) or exposure to heat to study the changes due to heating, exposure to gases or solutions, ion beam implant, etc.

The analysis is done by irradiating a sample with x-ray to ionize atoms and releasing photoelectrons. The XPS technique is highly surface specific due to the short range of the photoelectrons that are excited from the solid. It typically has the sampling depth of a few nanometers (1-10 nm usually). The energy of the photoelectrons leaving the sample are collected and analyzed by the instrument to produce a spectrum of emission intensity versus electron binding energy. Since the binding energy of the peaks is characteristic of each element, the peak areas can be used to determine the composition of the materials surface. Although XPS is a very useful technique used to determine what elements and the quantity of those elements that are presented in the sample surface, it still has some limitations. It takes relatively long time to survey scan and measure the

amount of all elements (1-10 minutes). Ultimate detection limit for most elements is approximately 100 part per million. Finally sample sizes need to be relatively big ranging between 1×1 to 3×3 cm.

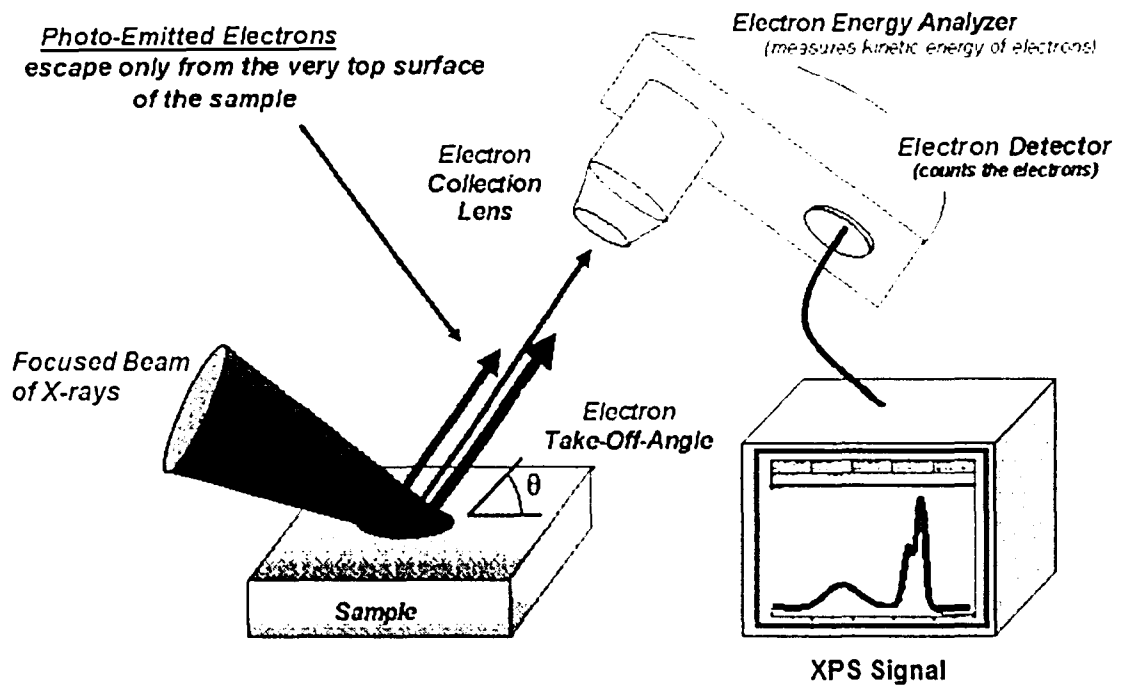


Figure 1-4. Basic components of XPS system*

* Picture from Wikipedia Encyclopedia (http://en.wikipedia.org/wiki/X-ray_photoelectron_spectroscopy)

1.5 Objectives

In this work, QWI effect induced by Cu-doped SiO_2 with Cu: SiO_2 film prepared by two different methods have been investigated. Methods that we used to introduce Cu impurity into the SiO_2 matrix are (i) Cu ion implantation, and (ii) Cu co-sputtering. The

co-sputtered Cu:SiO₂ was studied in parallel to compare the rate of intermixing with the ion-implantation technique.

1.6 Thesis outline

In this thesis, we document the development of a novel QWI process based on Cu:SiO₂. An introduction to the project and a brief review of QWI and process technology and metrology used in this research is given in Chapter 1. In Chapter 2, experimental procedures and the process technology are discussed. The experimental results, XPS results are presented in Chapter 3. The result discussion, conclusion and future work given in Chapter 4.

CHAPTER 2

EXPERIMENTAL PROCEDURES

This chapter documents the experimental procedures carried out for the GaAs/AlGaAs DQW, single quantum-well InGaP/GaAs red laser structure (633nm) and AlGaAs/GaAs quantum well laser structure (780nm).

The development of the QWI process used in this work began with the study of ion implantation. The GaAs/AlGaAs QWs based structure has been implanted with different concentration of Cu ion ranging in between 10^{12} cm^{-2} and 10^{15} cm^{-2} . Later the samples were then annealed at different temperature to study the ion implant parameters and anneal conditions effect the degree of intermixing. The implant species was chosen to be copper, because copper is known to be a deep level impurity and one of the fastest diffusing species in Si and dielectric materials, including SiO_2 when subjected to moderate temperature [19]. However, a concern with excessive copper is that the interaction between Cu and the dielectric may result in the electrical degradation of the insulator, loss of adhesion, or copper may diffuse into active device areas and degrade device performance.

Second, the co-sputtered Cu: SiO_2 was studied using the similar procedure to observe to intermixing. Sputtered silica process has been widely known as a promising and reliable approach to universally tune various of bandgap of quantum nanoheterostructures (i.e. quantum well and quantum dot). However, the mechanism of the sputtered silica process is not well understood. Also, the present knowledge is

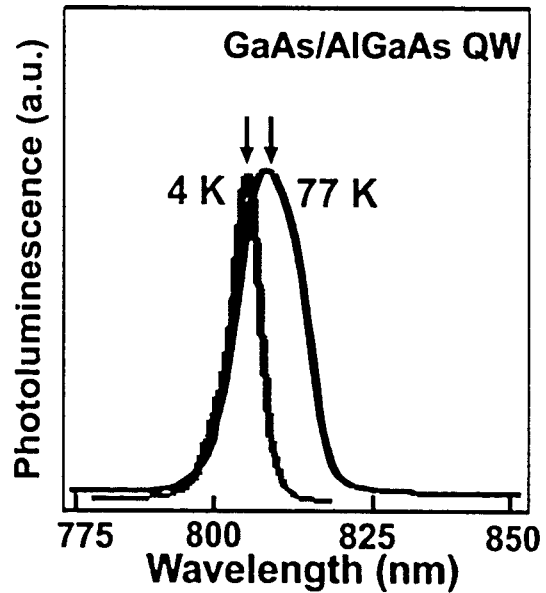
insufficient to explain why the intermixing effect occurs at relatively low activation energy as compared to other processes.

2.1 Sample structures

2.1.1 GaAs/AlGaAs DQW structure

The schematic diagram of the wafer structure and photoluminescence (PL) spectra of the GaAs/AlGaAs double quantum well structures used in this project are shown in Figure 2.1 a and 2.1 b respectively.

| Layers | Materials |
|----------------|--|
| Contact Layer | p+ GaAs |
| Graded | p-Al _{0.4} to Al _{0.0} |
| Upper Cladding | p-Al _{0.4} Ga _{0.6} As |
| Graded Barrier | Al _{0.2} Ga _{0.8} As |
| QW | GaAs |
| Barrier | Al _{0.2} Ga _{0.8} As |
| QW | GaAs |
| Graded Barrier | Al _{0.2} Ga _{0.8} As |
| Lower Cladding | n-Al _{0.4} Ga _{0.6} As |
| Buffer | n-GaAs |
| Substrate | n+GaAs |



(a)

(b)

Figure 2-1 (a) The schematic representation of the GaAs/AlGaAs DQW layer structure and (b) its Photoluminescence at 4K and 77K.

The GaAs/AlGaAs structure consists of two 10 nm well with 10 nm $\text{Al}_{0.2}\text{Ga}_{0.8}\text{As}$ barriers. The structure was completed by $\text{Al}_{0.4}\text{Ga}_{0.6}\text{As}$ lower cladding of 1.5 μm (with n-doping) and upper cladding of 1.5 μm (with p-doping). The contact layers consist of 100 nm p^+ GaAs and 100 nm n^+ GaAs. The samples gave a PL wavelength peak at 810 ± 10 nm at 77K.

2.1.2 Single Quantum-well InGaP/GaAs red laser structure (633nm)

The schematic diagram of the single quantum well InGaP/GaAs red laser wafer structure (633nm) used in this project are also shown in Figure 2.2 a and 2.2 b respectively. The InGaP/GaAs red laser structure consists of single quantum well with 50 nm $\text{GaIn}_x\text{P}_{1-x}$ barriers. The structure was completed by $\text{Al}_x\text{In}_{1-x}\text{P}$ lower cladding of 1 μm (with n-doping) and upper cladding of 1 μm (with p-doping). The contact layers consist of 200 nm p^+ GaAs and 200 nm n^+ GaAs.

| Layers | Materials |
|----------------|---------------------------------------|
| Contact Layer | p+GaAs |
| Upper Cladding | p-Al _x In _{1-x} P |
| Barrier | GaIn _x P _{1-x} |
| SQW | InGaP |
| Barrier | GaIn _x P _{1-x} |
| Lower Cladding | n-Al _x In _{1-x} P |
| Substrate | n+GaAs |

(a)

| | |
|-------------------------------------|---------|
| GaAs | 200 nm |
| Al _x In _{1-x} P | 1000 nm |
| GaIn _x P _{1-x} | 50 nm |
| InGaP QW | |
| GaIn _x P _{1-x} | 50 nm |
| Al _x In _{1-x} P | 1000 nm |
| GaAs | 300 nm |
| Substrate | |

(b)

Figure 2-2 (a) The schematic representation of the InGaP/GaAs SQW layer structure and (b) Schematic representation of the GaAs/AlGaAs SQW layer structure

2.2 Quantum Well Intermixing (QWI) mechanisms

Quantum well intermixing is a process in which atoms from quantum wells and their corresponding barriers interdiffuse, to alter the shape and depth of the quantum well, thus modifying the quantized energy state. In general, the interface between quantum well and barrier is metastable, in that under certain conditions, such as high temperature, the atoms in the quantum well and barrier will interdiffuse. Furthermore, the

compositional profile of QW is changed from a square to a parabolic profile due to the influence of injected impurities. After the interdiffusion process, the bandgap increases and the refractive index decreases. Therefore, blue shifts are possible to obtain from the process as long as the annealing temperature is below the thermal stability of the material.

2.3 Experimental Procedure

GaAs/AlGaAs DQW structure bare samples along with a 200 nm SiO₂ layer deposited samples using plasma enhanced chemical vapor deposition (PECVD) were used to investigate the IFVD effect. Three different dosages of $2 \times 10^{12} \text{ cm}^{-2}$, $5 \times 10^{13} \text{ cm}^{-2}$ and $2 \times 10^{15} \text{ cm}^{-2}$ copper ion implanted in GaAs/AlGaAs QWs samples were studied. After dielectric cap deposition and Cu-implantation, all samples were annealed under nitrogen ambient in a rapid thermal processor (RTP) at temperature between 700 °C and 950 °C for 2 minutes. During annealing, samples were sandwiched face-down between two pieces of fresh GaAs to prevent desorption of the Group V elements. The bare samples were also annealed as well to provide as the reference. During the annealing process, not only QW intermixing is promoted, but also recrystallizing the implanted layers will occur as well. The picture of the RTP used in this project is controlled by computer control unit and shown in Figure 2-3.

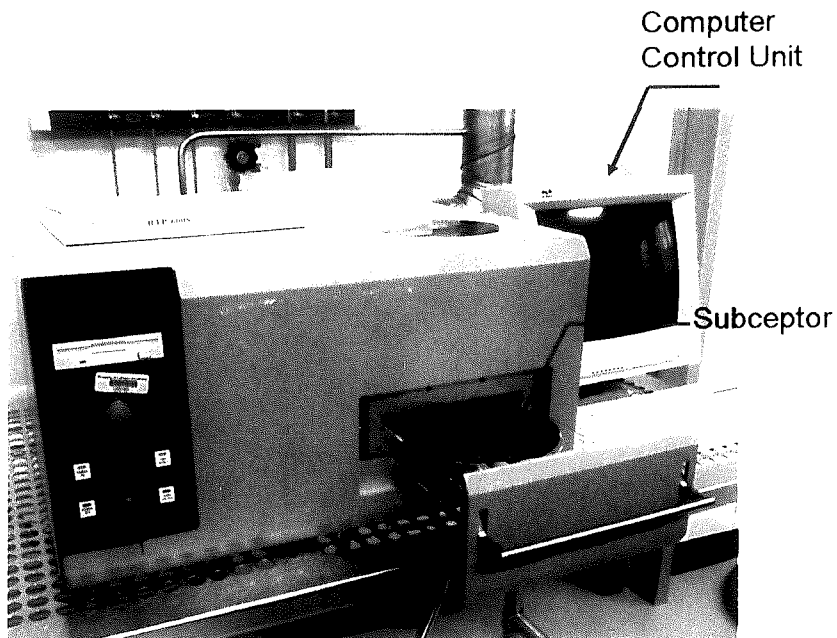


Figure 2-3. Rapid Thermal Processor (RTP) using in this project

After annealing, Photoluminescence (PL) spectroscopy was performed at 77 K using 532 nm diode pumped solid state laser as excitation source for GaAs/AlGaAs QWs. The schematic diagram of the PL setup used in this project is shown in Figure 2-4 and Figure 2-5.

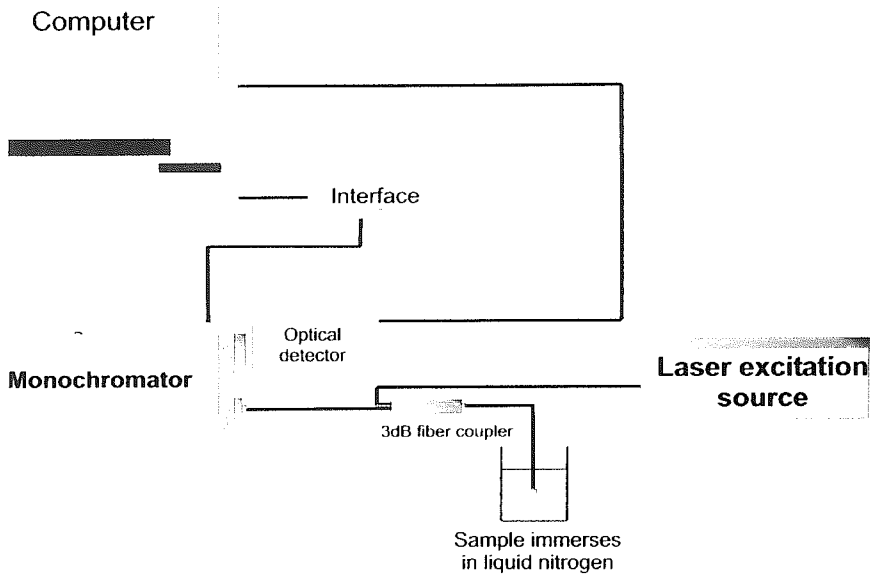


Figure 2-4. The schematic diagram of the 77K PL setup.

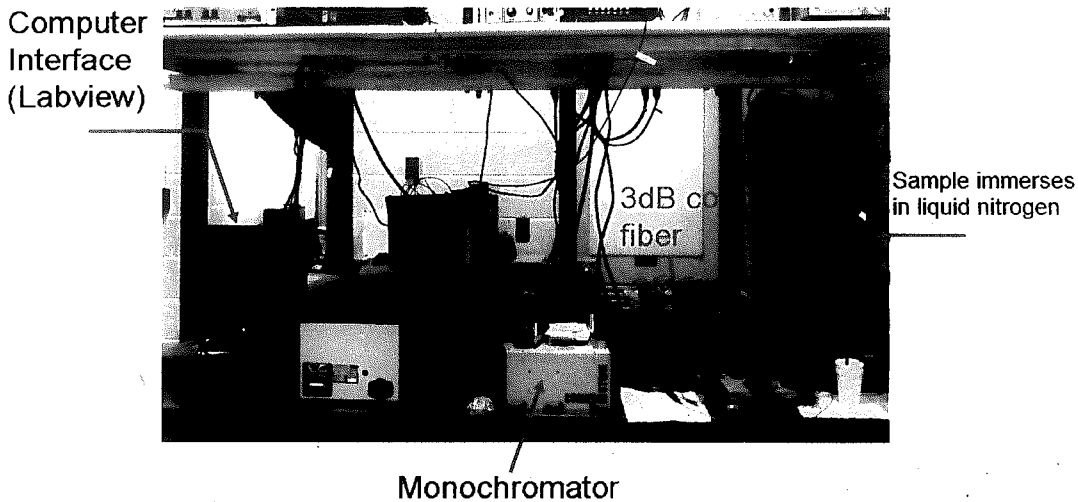


Figure 2-5. The 77K PL system

The as-grown material exhibits a single peak at 802 nm was use as a reference for GaAs/AlGaAs QWs. The 532 nm laser source is used for short wavelength (800 -1200 nm) PL measurement. The laser beam is focused into a 3 dB fiber coupler. The sample is mounted on top of the fiber and immersed into liquid nitrogen for 77K measurement. The luminescence from the sample is then collected by one end of the 3 dB coupler and guided into the monochromator. The PL spectrum is decomposed by an optical grating in an Oriel monochromator and is detected by a Si photodetector for short wavelength. Finally computer interface is being used to control the overall PL measurement.

2.3.1 Sputtering Setup

Copper sputtered silica process is also studied in parallel to compare the degree of intermixing caused by copper. About the same thickness of 200 nm sputtered SiO₂ was deposited upon GaAs/AlGaAs samples, single quantum-well InGaP/GaAs red laser structure (633nm) and GaAs/AlGaAs quantum well laser structure (780nm) samples. Both InGaP/GaAs red laser (633nm) and AlGaAs/GaAs quantum well laser (780nm) samples come with thin 120 nm silicon oxide layer on the top surface. Before Sputtering process, we use buffer HF to remove the silicon oxide layer. Later the deposition of ~ 200 nm Cu:SiO₂ was re-deposited.

The schematic diagram of the sputtering setup used in this project shown in Figure 2-6 consists of the following subsystems: a) the sputter chamber, in which the substrate holder and sputtering target reside; b) vacuum pumps to keep the chamber

under the vacuum of 2×10^{-3} Torr; c) RF power supplies; d) sputtering gas supply (Argon) and the flow controller; and finally the monitoring equipments which are pressure and voltage gauges.

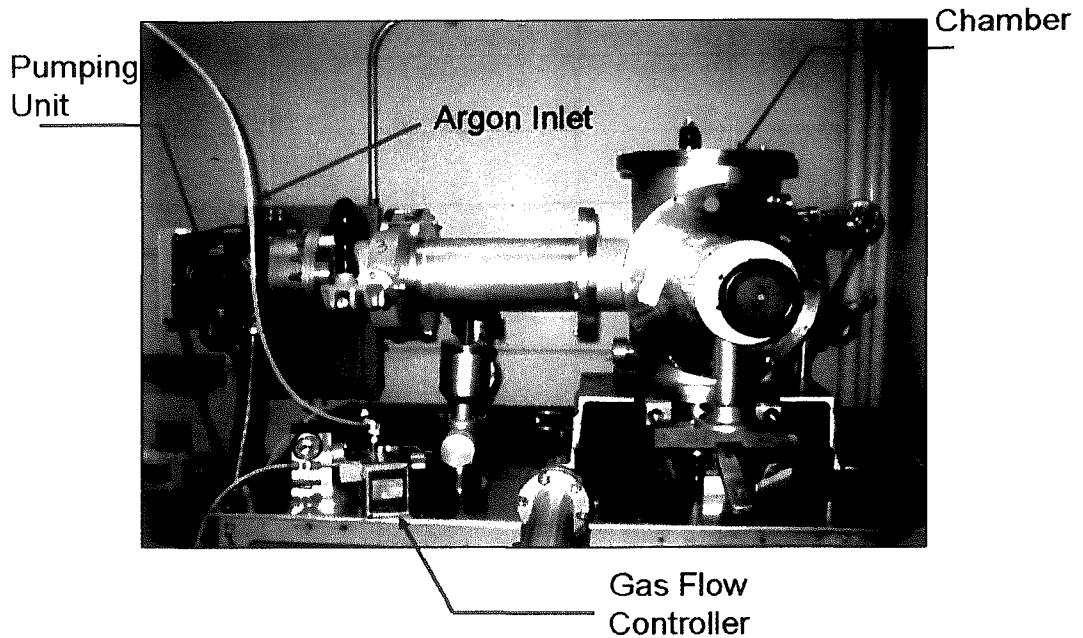


Figure 2-6. The sputtering system.

Thickness of the silica cap layer can be controlled by sputtering time. An Alpha Step Surface Profiler was used to determine the thickness of the sputtered silica film. An average sputtering rate of about 1.7 nm per minute was obtained from our process. Figure 2-7 show the picture of the Alpha step surface profiler.

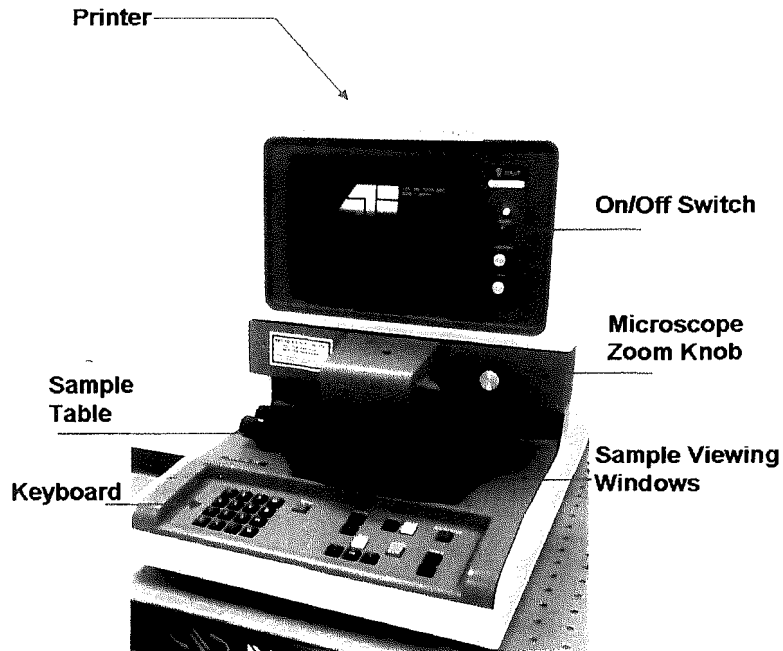


Figure 2-7. Alpha Step Surface Profiler.

The SiO₂ film deposition was carried out at a RF power 100 Watts and under vacuum, using Ar gas to generate the sputtering plasma. Pure semiconductor grade copper sputtering targets (purity > 99.99%) were placed on top of quartz plate in the center of the chamber. During sputtering process, the pressure inside the chamber is controlled to be at 2×10^{-3} Torr.

After the sputtering process, the samples were then annealed in a rapid thermal processor (RTP) at temperatures ranging between 700 °C and 950 °C for 2 mins. During annealing process, the same procedures as the copper implantation samples were carried out. Again, after annealing, same PL spectroscopy was performed to determine the

bandgap shift using 533 nm laser as excitation source. However, for InGaP/GaAs red laser (633nm), 444nm blue laser was used as an excitation source instead of the 532 nm.

2.4 Summary

In this chapter, the schematic representations of GaAs/AlGaAs DQW, single quantum-well InGaP/GaAs red laser structure (633nm) and AlGaAs/GaAs quantum well laser structure (780nm) used in this project and mechanism of QWI were explained. We then discussed the experimental procedures for ion implantation and Cu co-sputtering in detail.

CHAPTER 3

RESULTS

In this chapter, the experimental results performed in chapter 2 are reported. Two different methods that we used to introduce Cu impurity into the SiO₂ matrix are (i) Cu ion implantation, and (ii) Cu co-sputtering. The PL results from the Cu ion implantation were first discussed follows by the co-sputtered Cu:SiO₂ PL results. Lastly, XPS results that carried out to study the diffusivity of copper before and after the rapid thermal annealing process were discussed.

3.1 Cu-ion Implantation Results

No bandgap shifts were obtained from any of the different ion implanted GaAs/AlGaAs QWs samples when annealed at 850 °C and also no significant shifts were obtained at the annealed temperatures below 925 °C. Moreover, the results show that the samples that were implanted with $2 \times 10^{12} \text{ cm}^{-2}$ Cu-ion yielded the largest bandgap shift follows by $5 \times 10^{13} \text{ cm}^{-2}$ and $2 \times 10^{15} \text{ cm}^{-2}$ respectively (Figure 3-1 , Figure 3-2 and Figure 3-3). After annealing at 950 °C, the effect of intermixing started to play a significant role since a bandgap shift of 56 meV (28nm) and 20 meV (10nm) has been measured from the GaAs/AlGaAs QWs SiO₂ capped and the bare samples respectively. The differential bandgap shift between the GaAs/AlGaAs QWs SiO₂ capped and the bare surface samples becomes significant (i.e. 56 meV) after annealing at 925°C. suggesting that the IFVD

effect mediated by the Ga vacancies begins to dominate. Finally the energy bandgap shift of all the GaAs/AlGaAs QWs samples were compared and shown in Figure 3-4.

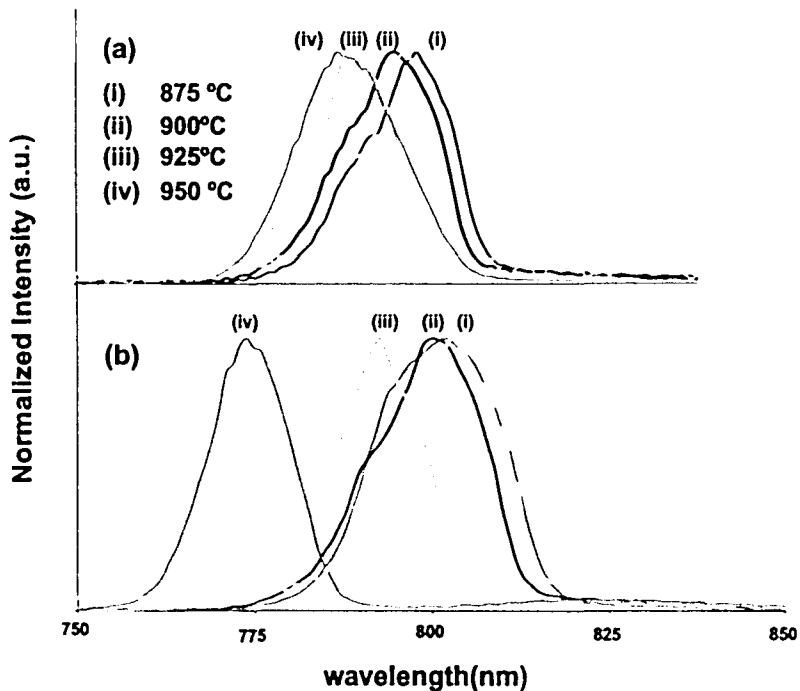


Figure 3-1. The PL spectra at 77K after rapid thermal annealing at various temperatures [(i) 875 °C, (ii) 900 °C, (iii) 925 °C, and (iv) 950 °C] from (a) the bare (note that the spectrum of as-grown is included as the dotted line), (b) SiO₂ capped $2 \times 10^{12} \text{ cm}^{-2}$ of copper ion implanted GaAs/AlGaAs QWs material.

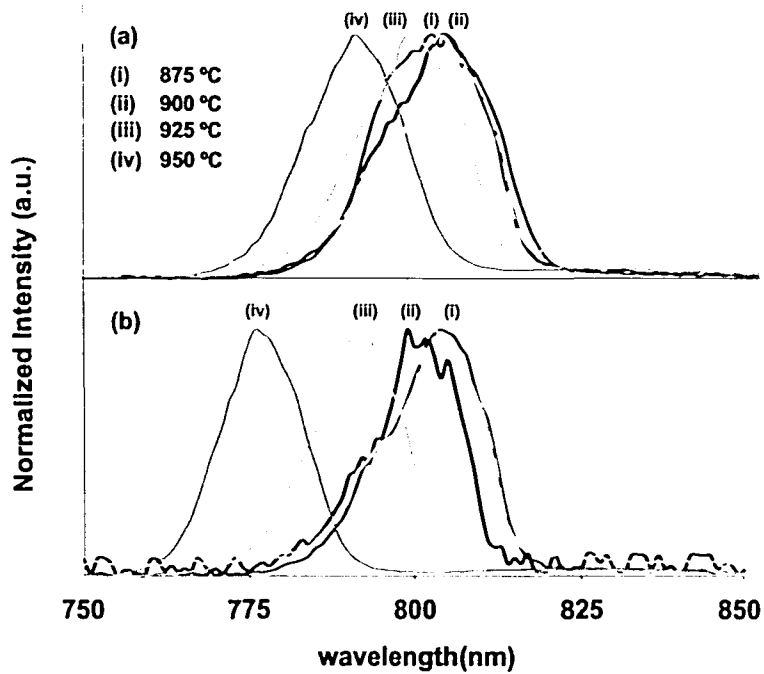


Figure 3-2. The PL spectra at 77K after rapid thermal annealing at various temperatures [(i) 875 °C, (ii) 900 °C, (iii) 925 °C, and (iv) 950 °C] from (a) the bare (note that the spectrum of as-grown is included as the dotted line), (b) SiO₂ capped $5 \times 10^{13} \text{ cm}^{-2}$ of copper ion implanted GaAs/AlGaAs QWs material.

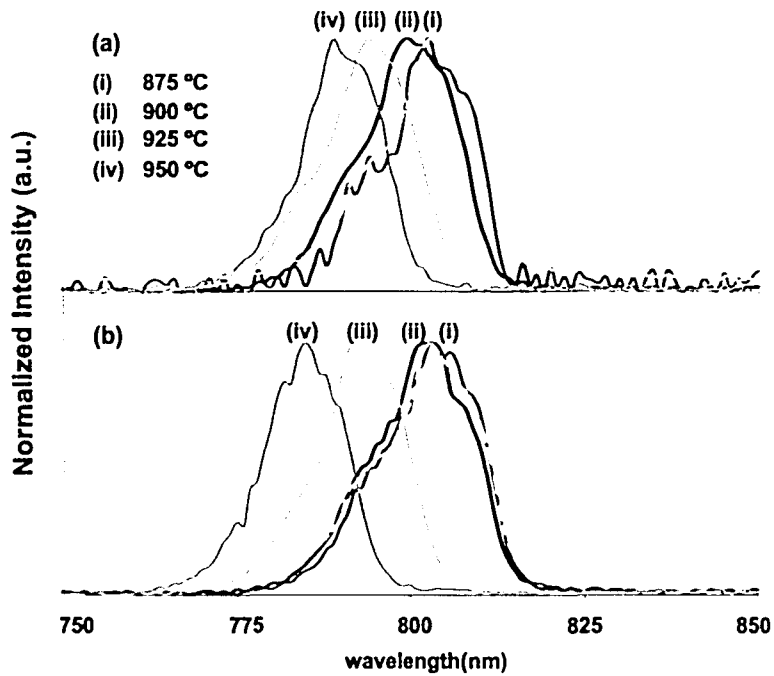


Figure 3-3. The PL spectra at 77K after rapid thermal annealing at various temperatures [(i) 875 °C, (ii) 900 °C, (iii) 925 °C, and (iv) 950 °C] from (a) the bare (note that the spectrum of as-grown is included as the dotted line), (b) SiO₂ capped $2 \times 10^{15} \text{ cm}^{-2}$ of copper ion implanted GaAs/AlGaAs QWs material.

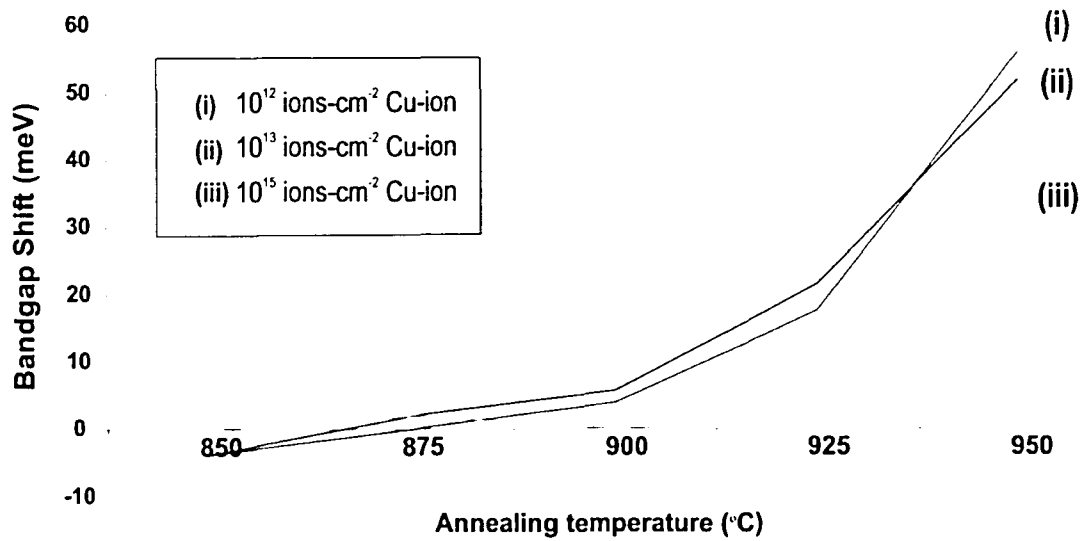


Figure 3-4. The PL energy shifts measured at 77K versus annealing temperature from SiO₂ capped GaAs/AlGaAs QWs samples at various copper dosages.

In summary for the results from ion implantation, we observed that the implanted samples gave similar PL spectrum shape as compared to as-grown sample, this implies that the quality of the implanted materials remain good after QWI.

3.2 Cu:SiO₂ Sputtering Results

Since the results from the ion implantation show that copper which is one of the fastest electrically elements can be used to promote the degree of intermixing in the GaAs/AlGaAs QWs therefore, the co-sputtered Cu:SiO₂ were studied as to compare to the implantation process.

Unlike the result from the copper ion implantation, sputtered silica shows the tremendous blue shift in bandgap energy. The shifts rapidly increase with increasing annealing temperature. Figure 3-5 shows when the samples were annealed at 875°C the bandgap shift of 153 meV (72nm) was observed and keep increasing as the annealing temperature increased. Finally, the bandgap shift of 270 meV (119nm) was obtained at annealing temperature equals to 950°C from the GaAs/AlGaAs QWs samples.

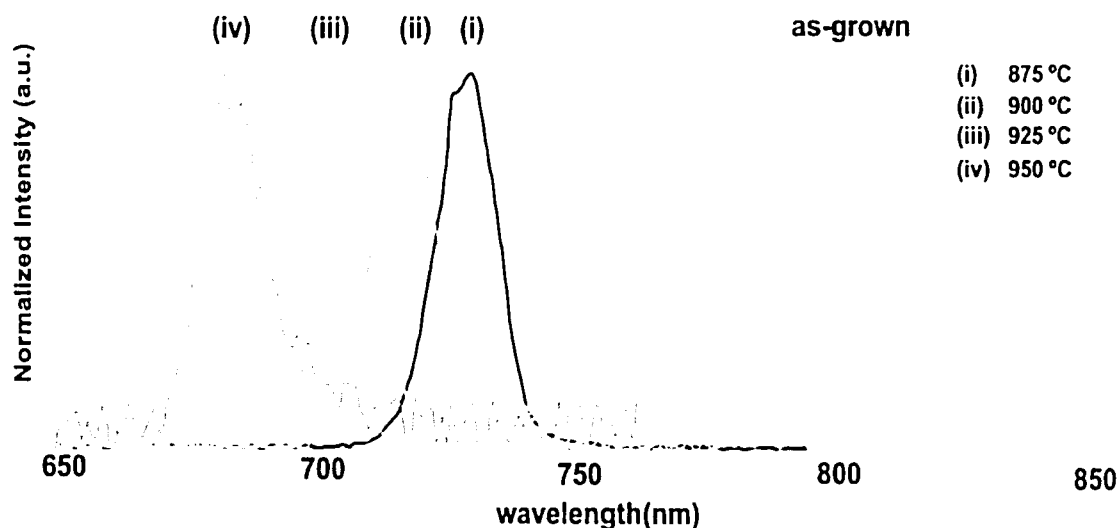


Figure 3-5. The PL spectra at 77K after rapid thermal annealing at various temperatures [(i) 875 °C, (ii) 900 °C, (iii) 925 °C and (iv) 950 °C (note that the spectrum of as-grown is included as the dotted line)] from co-sputtered Cu:SiO₂ GaAs/AlGaAs QWs materials.

The results of this study show that the use of sputtered compare to PECVD SiO₂ clearly leads to a substantial lowering of the threshold temperature for intermixing. We suspect that during the sputtering process, the atomic bombardment causes the creation of point defects on the sample surface, which induced the intermixing process. Therefore,

the increasing of point defect densities compare to PECVD SiO₂, help to promote the outdiffusion of Ga and induffision of Copper into the substrate [2].

Subsequently we demonstrate the co-sputtered silica onto the single quantum-well InGaP/GaAs red laser (633nm) structure and GaAs/AlGaAs quantum well laser structure (780nm) samples. Both InGaP/GaAs red laser (633nm) and AlGaAs/GaAs quantum well laser (780nm) samples come with thin Silicon oxide layer on the top surface. Before sputtering process, we use 1:10 ratio (water: HF) buffer HF to remove the silicon oxide layer. A good surface morphology was obtained after the removal of the SiO₂. Later the deposition of ~ 200 nm Cu:SiO₂ was re-deposited. After gone through the same annealing process as the double quantum well GaAs/AlGaAs samples, photoluminescence were performed under 77K for both single quantum well InGaP/GaAs red laser (633nm) and GaAs/AlGaAs quantum well laser (780nm) using 444 nm blue laser and 533 nm laser as excitation sources respectively.

Figure 3-6 shows the 77K PL spectrum from single quantum well InGaP/GaAs red laser (633nm) structure using 444nm blue laser as an excitation light source. It shows the PL shift was being able to obtain from InGaP/GaAs red laser at various temperatures. The largest differential PL shift of 150 meV (41nm) has been measured at 900 °C, while there is only a small shift of 25 meV (8nm) obtained from sample annealed at the starting temperature of 800 °C. We also find out the PL shift start to decrease when sample annealed above 900 °C that is at 925 °C, this may be because of too high temperature annealing has already damaged the material quality. However, no significant broadening

in PL linewidth after annealing has been observed, which indicates that the optical quality of the samples is not affected by the intermixing process.

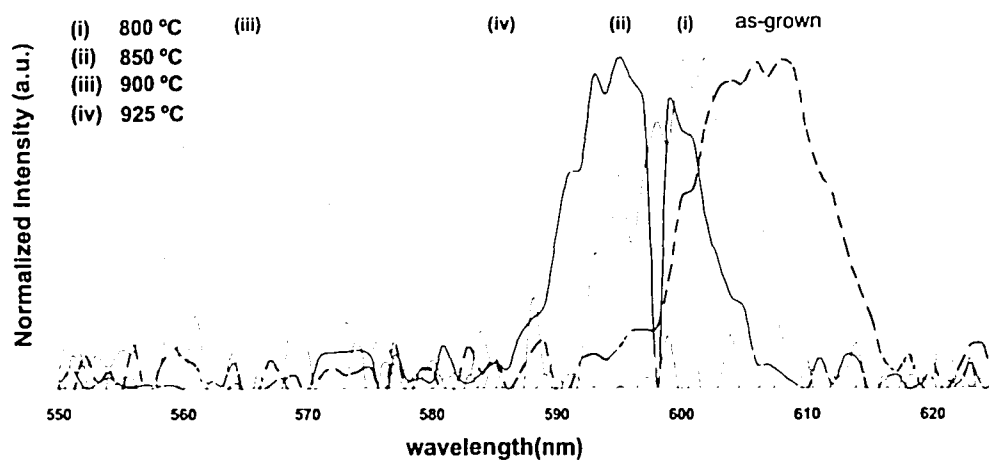


Figure 3-6. The PL spectra at 77K after rapid thermal annealing at various temperatures [(i) 800 °C, (ii) 850 °C, (iii) 900 °C, and (iv) 925 °C] from co-sputtered Cu:SiO₂ single quantum well InGaP/GaAs red laser structure.

Similarly for the AlGaAs/GaAs quantum well laser (780nm) sample, the shift of PL peak is negligible at beginning temperature of 700 °C. However, PL peak shift keeps increasing up to 152 meV (61nm) shift when annealing temperature goes up to 800 °C. Since there was no evidence PL linewidth change, we can draw a conclusion that the optical quality of the material was still not affected by intermixing process as well.

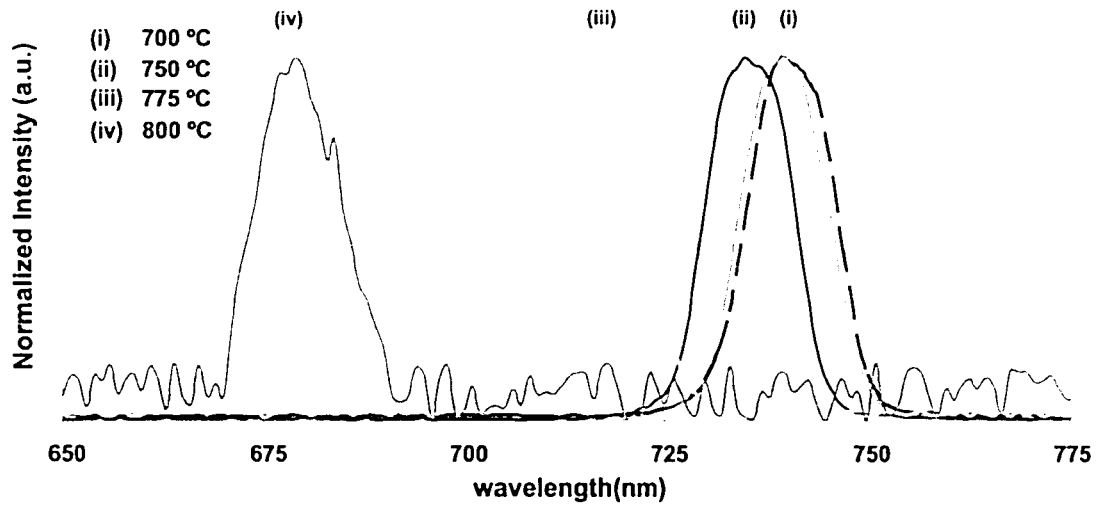


Figure 3-7. The PL spectra at 77K after rapid thermal annealing at various temperatures [(i) 700 °C, (ii) 750 °C, (iii) 775 °C, and (iv) 800 °C] from co-sputtered Cu:SiO₂ AlGaAs/GaAs quantum well laser structure (780nm).

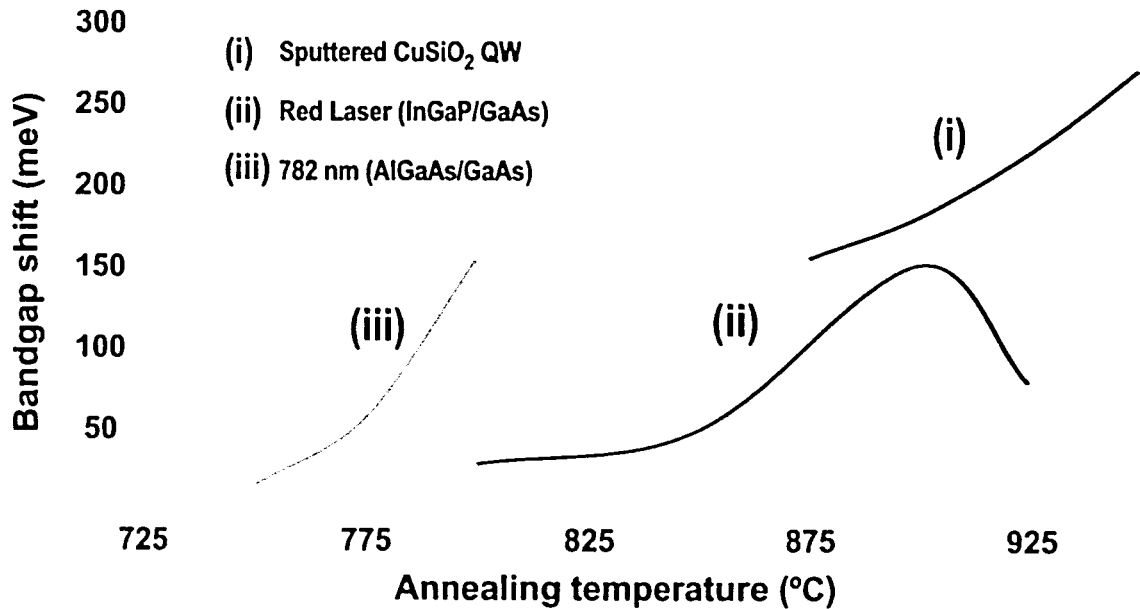


Figure 3-8. The PL energy shifts measured at 77K versus annealing temperature from sputtered GaAs/AlGaAs QW, single quantum well InGaP/GaAs red laser, and AlGaAs/GaAs quantum well laser (780nm) materials..

From Figure 3-8, bandgap energy shifts obtained from GaAs/AlGaAs QW, single quantum well InGaP/GaAs red laser material, and AlGaAs/GaAs quantum well laser (780nm) were plotted together. It is obviously see that all the co-sputtered samples have presented an influential shift of bandgap energy compared to the implanted samples shown in Figure 3-4 at the same annealing temperatures. This implies that Cu:SiO₂ sputtering process has lower activation energy for intermixing process compare to the ion implantation process.

Based on the overall results of this study, although we observed the enhanced bandgap shift with no evidence of the saturation of the intermixing rate as the copper dose increased, the results imply that with too high dosage of copper ion implantation may cause the higher diffusivity of copper, hence degrade the degree of intermixing. The lowest dosage of copper ion at 2×10^{12} ions-cm⁻² gave the highest degree of intermixing and decrease respectively as the dosage increased. However, the use of sputtered silica compare to PECVD SiO₂ clearly leads to a substantial lowering of the threshold temperature for intermixing. During the sputtering process, the atomic bombardment causes the creation of point defects on the sample surface, which induced the intermixing process. Therefore, the increasing of point defect densities compare to PECVD SiO₂, help to promote the outdiffusion of Ga and induffsiion of Copper into the substrate [2]. Consequently, reduces the temperature used to promote the same degree of intermixing and does not effect the optical properties of the material due to insignificant linewidth change.

3.3 X-ray Photoelectron Spectroscopy (XPS) Results

In this experiment, the XPS was carried out to study the diffusivity of copper before and after the rapid thermal annealing process. Especially, when after annealing process, we expected to observe the diffusion of copper penetrates into the substrate and as the result promoting the intermixing effect.

Figure 3-9 (a) and (b) shows the XPS result directly after implanted copper ion into the GaAs based bare sample without process through the thermal process. The results show that there is a number of copper composition accumulation at the surface of the sample since the penetration limitation of XPS is only a few up to ten nanometers near the surface. However, after process the sample through rapid thermal annealing process of 800 °C, we were barely be able to observe any composition of copper from the same sample as shown in Figure 3-10 (a) and (b). Since the binding energy of the copper is around 932-933 eV, the result shown in Figure 3-10 (b) can be interpreted in the way such that copper was not be able to observe from the sample surface anymore. This result confirms that copper ion has been diffused into the material after process through rapid thermal annealing.

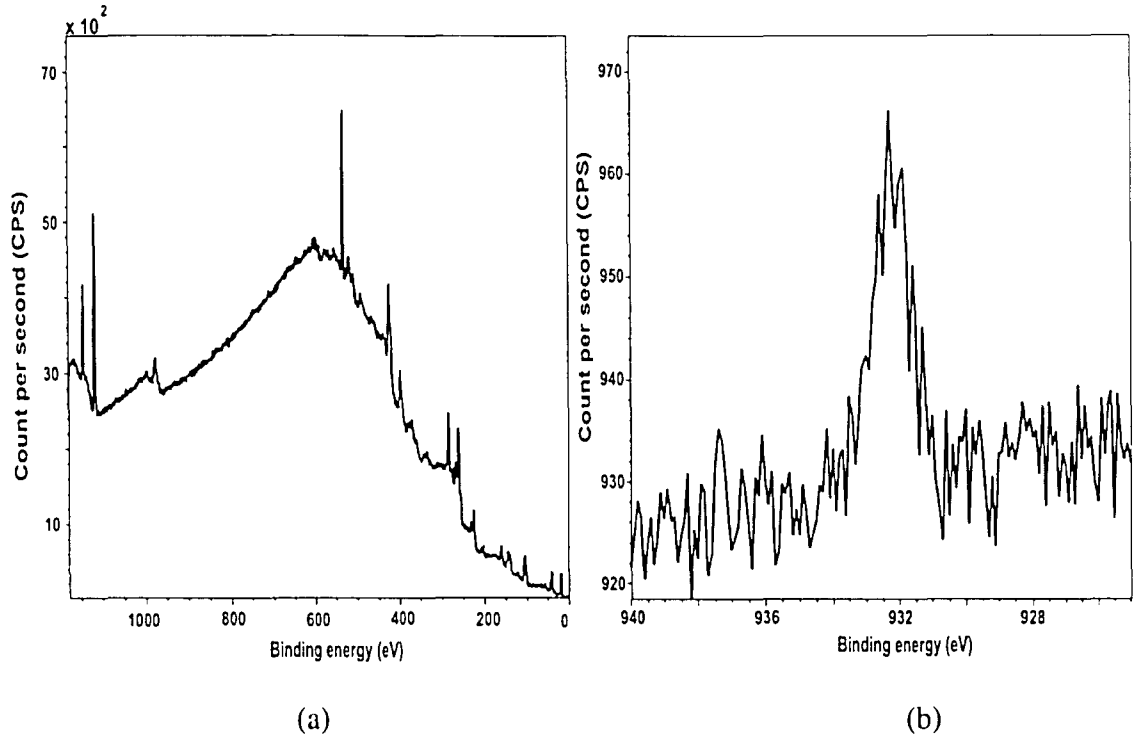


Figure 3-9. X-ray Photoelectron Spectroscopy from copper implanted GaAs based bare samples before rapid thermal annealing. (a) Overall signal from the sample (b) Zoom in binding energy peak obtains from copper element (note that copper binding energy peak is around 932-933 eV).

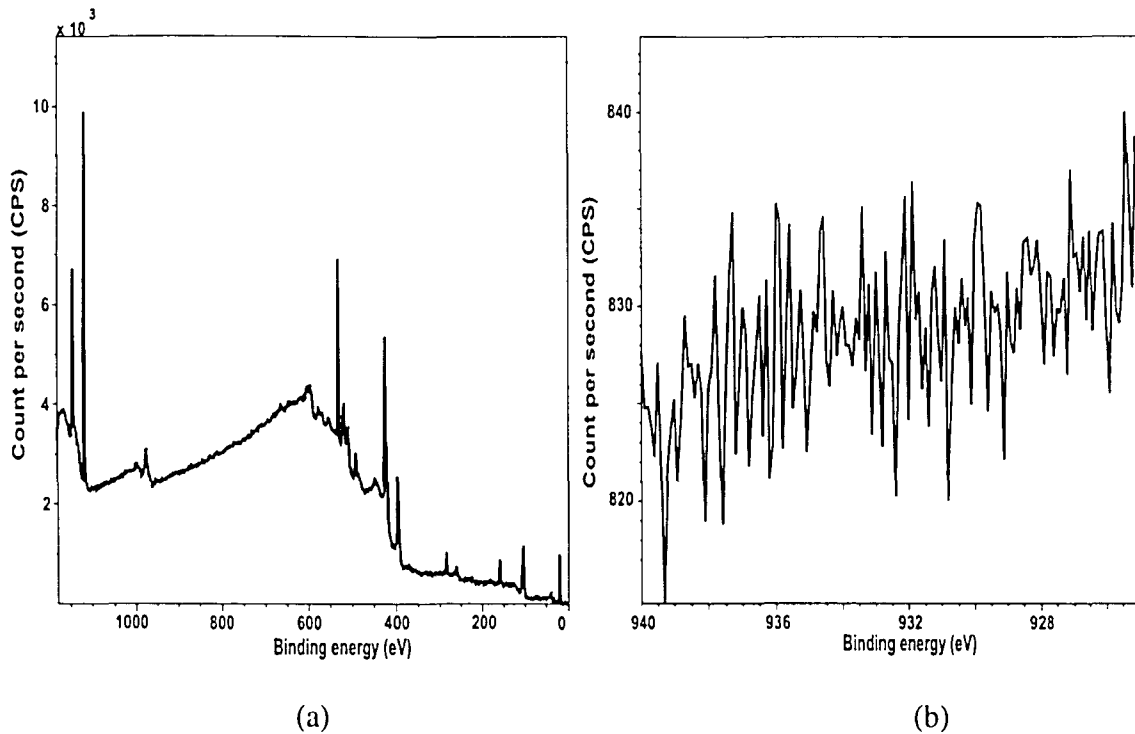


Figure 3-10. X-ray Photoelectron Spectroscopy from copper implanted samples after rapid thermal annealing. (a) Overall signal from the sample (b) Zoom in binding energy peak obtains from copper element (932-933 eV).

Similarly, Figure 3-11 (a) and (b) and Figure 3-12 (a) and (b) show that the same phenomenon have also taken place in our Cu:SiO₂ co-sputtered process. However, before XPS measuring, we have removed the SiO₂ layer out by using buffer HF in order to be able to detect stronger signal from the sample.

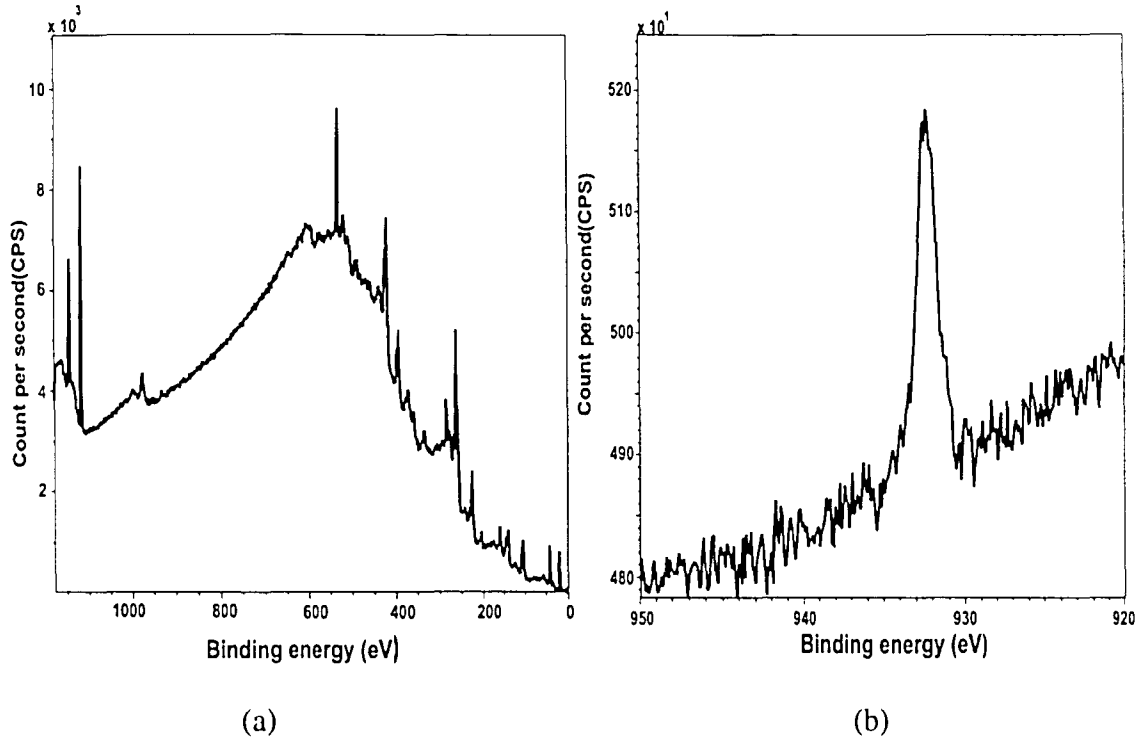


Figure 3-11. X-ray Photoelectron Spectroscopy from co-sputtered Cu:SiO₂ samples after removing SiO₂ layer before rapid thermal annealing. (a) Overall signal from the sample (b) Zoom in binding energy peak obtained from copper element (932-933 eV).

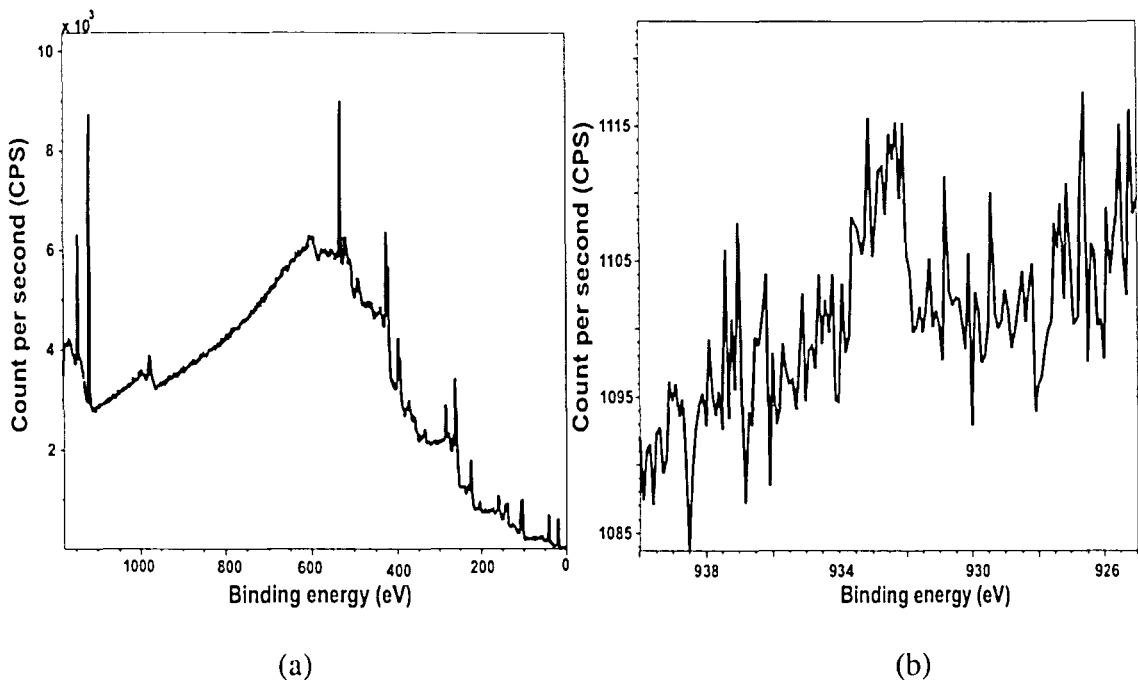


Figure 3-12. X-ray Photoelectron Spectroscopy from co-sputtered Cu:SiO₂ samples after removing SiO₂ layer after rapid thermal annealing. (a) Overall signal from the sample (b) Zoom in binding energy peak obtains from copper element (932-933 eV).

3.4 Summary

In this chapter, the possible influence of impurity incorporation into the silica cap during implantation and sputtered silica process on the enhancement of intermixing of quantum nanostructure at low activation energy has been systematically investigated. In our study, we found that the incorporation of a small percentage of copper into the silica film essentially enhance the degree of intermixing. The interdiffusion rate can be controlled by incorporating different concentration of copper in the silica cap. Various QW heterostructures such as GaAs/AlGaAs DQW, single Quantum-well InGaP/GaAs red

laser structure (633nm) and AlGaAs/GaAs quantum well laser structure (780nm) were used in the copper-doped sputtered silica process and observed the shifts of the bandgap energy. Although, implantation which is a reproducible process shows to promote intermixing in GaAs/AlGaAs material system, still cannot compare to the results that were obtained from the sputtering process.

A differential wavelength shift of as large as 119 nm (i.e. 270 meV) was observed from sputtered Cu:SiO₂ GaAs/AlGaAs QWs material system without any significant change in linewidth. Furthermore our XPS measurement confirms that the diffusion of copper has taken place into the material after rapid thermal process. Based on the previous result of the bandgap energy shift, it implies that intermixing process has occurred. Therefore, we conclude that the diffusion of copper ion into the material help elevated the degree of intermixing through both IID and IFVD processes.

In summary, from these results, we conclude that a good quality material can be obtained using this Cu:SiO₂ sputtering process and suggest that this technology is a promising universal intermixing technique for the planar integration of multiple active/passive quantum heterostructure based devices on a single chip in the future.

CHAPTER4

DISSCUSSION AND CONCLUSION

In this chapter, we first discuss the experimental results from Chapter 3. Then follow by the conclusion of this thesis work and the recommendation for future works.

4.1 Discussion

Based on the overall results of this study, although from our result we observed the enhanced bandgap shift with no evident of the saturation of the intermixing rate as the copper dose increased. The results imply that with too high dosage of copper ion implantation may cause the higher diffusivity of copper, hence degrade the degree of intermixing since the lowest dosage of copper ion at $2 \times 10^{12} \text{ cm}^{-2}$ gave the highest degree of intermixing and decrease respectively as the dosage increased. However, the use of sputtered silica compare to PECVD SiO_2 clearly leads to a substantial lowering of the threshold temperature for intermixing. During the sputtering process, the atomic bombardment causes the creation of point defects on the sample surface, which induced the intermixing process. Therefore, the increasing of point defect densities compare to PECVD SiO_2 , help to promote the outdiffusion of Ga and induffision of Copper into the substrate. Consequently, reduces the temperature used to promote the same degree of intermixing and does not effect the optical properties of the material due to insignificant linewidth change.

4.2 Conclusion

We have successfully developed a versatile postgrowth bandgap engineering technology for GaAs based quantum nanostructures. Both copper ion implantation and Cu:SiO₂ sputtering processes develop in this thesis work can control the degree of bandgap energy shift in wide range of GaAs based quantum well materials. Differential bandgap shifts between the un-implanted and implanted regions as large as 56 meV (28nm) has been observed from the copper implanted sample with a dosage of 2×10^{12} ions-cm⁻². However, the differential bandgap shifts between the GaAs/AlGaAs DQW bare samples and the Cu:SiO₂ sputtered samples of over 270 meV (119nm) was observed. Moreover, from the PL results we were barely observed any significant change in linewidth, this indicates that the quality of the material remains good after quantum well intermixing (QWI).

From the X-ray Photoelectron Spectroscopy measurement, we have observed the diffusion of copper from the surface into the well regions of the sample, creating intermixing process. Based on the over all result of this work, we assure that Cu:SiO₂ induced QW is a promising and reliable technology for monolithic integration of GaAs based PICs.

4.3 Recommendation for Future works

For the next challenging step, it is recommended to demonstrate passive and active photonics device integration using Cu:SiO₂ intermixing technology. After that characterization of novel photonic integrated devices should be investigated.

Since this technique has only being apply to GaAs based quantum well structure, therefore applying Cu:SiO₂ intermixing technology with other materials such as InP based materials, and other quantum heterostructures such as quantum dots and quantum dash-in well will be significant. Later, demonstrations of passive and active photonics devices using CuSiO₂ intermixing technology from these quantum heterostructures will complete the approach of monolithic integrated devices.

REFERENCES

- [1] J. H. Marsh, "Quantum well intermixing", *Semicond. Sci. Technol.*, **8**, p. 1136-1155, 1993.
- [2] O.P. Kowalski, C.J. Hamilton, S.D. McDougall, J.H. March, A.C. Bryce, R.M. De La Rue, B. Vögele, and C. R. Stanley, "A Universal damage induced technique for quantum well intermixing", *Appl. Phys. Lett.*, **72**, p. 581-583, 1998.
- [3] N. Holonyak, Jr., "Impurity-Induced Layer Disordering of Quantum-Well Heterostructures: Discovery and Prospects", *IEEE J. Selected topics in Quan. Electr.*, **4**, p. 584-594, 1998.
- [4] S.D. McDougall, O.P. Kowalski, C.J. Hamilton, F. Camacho, B. Qiu, M. Ke, R. M. De La Rue, A. C. Bryce and J. H. Marsh, "Monolithic Integration via a Universal Damage Enhanced Quantum-Well Intermixing Technique", *IEEE J. Selected topics in Quan. Electr.*, **4**, p. 636-646, 1998.
- [5] B. Elman, E. S. Koteles, P. Melman, and C. A. Armiento, "GaAs/AlGaAs quantum-well intermixing using shallow ion implantation and rapid thermal annealing", *J. Appl. Phys.*, **66(5)**, p. 2104-2107, 1989.
- [6] W. D. Laidig, N. Holonyak, Jr., M. D. Camras, K. Hess, J. J. Coleman, P. K. Kapkus, and J. Bardeen, "Disordering of an AlAs-GaAs superlattice by impurity diffusion", *Appl. Phys. Lett.*, **38**, p.776, 1981.
- [7] D. G. Deppe, and N. Holonyak, Jr., "Atom diffusion and impurity-induced layer disordering in quantum well III-V semiconductor heterostructures", *J. Appl. Phys.*, **64**, R93, 1988.
- [8] B. S. Ooi, C. J. Hamilton, K. McIlvaney, A. C. Bryce, R. M. De La Rue, J. H. Marsh, and J. S. Roberts, "Quantum-Well Intermixing in GaAs-AlGaAs Structures Using Pulsed Laser Irradiation", *Photon. Tech. Lett.*, **9**, p. 587-589, 1997.
- [9] B. S. Ooi, A. C. Bryce, J. H. Marsh, and J. S. Roberts, "Effect of p and n doping on neutral impurity and SiO₂ dielectric cap induced quantum well intermixing in GaAs/AlGaAs structures", *Semicond. Sci. Technol.*, **12**, p. 121-127, 1997.
- [10] H. S. Djie, C. K. F. Ho, T. Mei, and B. S. Ooi, "Quantum well intermixing enhancement using Ge-doped sol-gel derived SiO₂ encapsulant layer in InGaAs/InP laser structure", *Appl. Phys. Lett.*, **86**, p.081106-1, 2005.

- [11] B. C. Qiu, A. C. Bryce, R. M. De La Rue, and J. H. Marsh, "Monolithic Integration in InGaAs-InGaAsP Multiquantum-Well Structure Using Laser Processing", *Photon. Tech. Lett.*, **10**, p. 769-771, 1998.
- [12] A. S. Helmy, S. K. Murad, A. C. Bryce, J. S. Aitchison, J. H. Marsh, S. E. Hicks, and C. D. W. Wilkinson, "Control of silica cap properties by oxygen plasma treatment for single-cap selective impurity free vacancy disordering", *Appl. Phys. Lett.*, **74**, p. 732-734, 1999.
- [13] S. K. Si, D. H. Yeo, K. H. Yoon, and S. J. Kim, "Area Selectivity of InGaAsP-InP Multiquantum-Well Intermixing by Impurity-Free Vacancy Diffusion", *IEEE J. Selected topics in Quan. Electr.*, **4**, p. 619-623, 1998.
- [14] J. K. Choi, J. Lee, J. B. Yoo, J. S. Maeng, and Y. M. Kim, "Residual stress analysis of SiO₂ films deposited by plasma-enhanced chemical vapor deposition", *Surface and Coatings Tech.*, **131**, p. 153-157, 2000.
- [15] K. N. Srijith, V. Ranjit, B. S. Ooi, Y. C. Chan, Y. L. Lam, and C. H. Kam, "Fabrication And Characterization of Bandgap Tuned Lasers in GaAs/AlGaAs Quantum Well Structures Using Pulsed Laser Irradiation"
- [16] S. M. Rossnagel, "Sputter deposition for semiconductor manufacturing", *IBM J. Research and Development*, **43(1/2)**, p. 163-179, 1999.
- [17] S. Rogojevic, A. Jain, W. N. Gill, and J. L. Plawsky, "Interactions Between Nanoporous Silica and Copper", *J. The Electrochemical Society*, **149**, p. F123, 2002.
- [18] W. F. McArthur, K. M. Ring, K. L. Kavanagh, "Cu Diffusion and Structural Degradation of Amorphous Metal Silicon Nitride Barriers For ULSI Interconnects"

VITA

Vitchanetra Hongpinyo was born in July 1982, in Bangkok, Thailand, Born to be the oldest child and the middle for two brothers in the family of Dr. Voradej and Mrs. Hattaya Hongpinyo. After graduating high school from Satriwitthaya, she spent four years for her bachelor degree at Chulalongkorn University, Thailand, majored in Telecommunication System of Electrical Engineering Department. Right after she finished her Bachelor Degree in March 2004, she started working at Fabrinet Company from May 2004 to June 2005. Operating as a test engineer at a high-tech optical communication electronic company and accounting for Emcore Ortel Optic and JDS Uniphase's products has enabled her to utilize her technical and interpersonal skills in new challenging ways. Her role was responsible for test stations and analyzed products' performances and failures and solved the problem to increase the yield rate in the production line. However, working in a company was not really her passion, she always wants to be in the teaching field, therefore in April 2005, she decided to move on and apply for Master Degree at Lehigh University, USA. Currently she is a graduate student in Electrical and Computer Engineering Department working under Associate Professor. Boon Siew Ooi's research group. After graduating with Master of Science degree in May 2007, she continues her study toward Ph.D degree at Lehigh University.

END OF TITLE